(University of Toronto Press, Toronto, Canada, 1960), p. 224.
[9]R. W. Benjamin, P. S. Buchanan, and I. L. Morgan, Nucl. Phys. 79, 241 (1966).
[10]J. R. MacDonald and M. A. Grace, Nucl. Phys. A92, 593 (1967).
[11]M. E. Phelps, D. G. Sarantites, and W. G. Winn, Nucl. Phys. A149, 647 (1970).
[12]D. C. Camp and G. L. Meredith, Nucl. Phys. A166, 349 (1971).
[13]Y. K. Agarawal, S. Hofman, and K. Wien, Nucl. Phys. A176, 142 (1971).
[14]A. H. Sher and B. D. Pate, Nucl. Phys. A112, 85 (1968).
[15]K. Vaughan, B. D. Pate, and M. H. Shapiro, Nucl. Phys. A130, 62 (1969).
[16]G. G. Seaman, N. Benczer-Koller, M. C. Bertin, and J. R. MacDonald, Phys. Rev. 188, 1706 (1969).
[17]N. Benczer-Koller, private communication.
[18]W. E. Kinney and F. G. Perey, Nucl. Sci. Eng. 40, 396 (1970).
[19]V. J. Orphan, C. G. Hoot, and J. John, Nucl. Sci. Engr. 42, 352 (1970).
[20]V. J. Orphan and C. G. Hoot, Gulf Radiation Technology Report No. Gulf-RT-A10743, 1971 (unpublished).
[21]C. A. Engelbrecht, Nucl. Instr. Methods 80, 187 (1970).
[22]E. Sheldon and D. M. Van Patter, Rev. Mod. Phys. 38, 143 (1966).
[23]J. K. Dickens and F. G. Perey, Oak Ridge National Laboratory Report No. ORNL-4592, 1970 (unpublished).
[24]W. Hauser and H. Feshbach, Phys. Rev. 87, 366 (1952).
[25]F. G. Perey and B. Buck, Nucl. Phys. 32, 353 (1962).
[26]E. Barnard, J. A. M. DeVilliers, C. A. Engelbrecht, D. Reitmann, and A. B. Smith, Nucl. Phys. A118, 321 (1968).
[27]V. C. Rogers, D. C. Hedengren, V. J. Orphan, and C. G. Hoot, Trans. Am. Nucl. Soc. 14, 897 (1971).
[28]A. Gilbert and A. G. W. Cameron, Can. J. Phys. 43, 1446 (1965).
[29]J. H. Towle and R. O. Owens, Nucl. Phys. A100, 257 (1967).
[30]J. Vervier, Nucl. Phys. 78, 497 (1966).
[31]J. B. McGrory, Phys. Rev. 160, 915 (1967).
[32]G. S. Mani, Nucl. Phys. A165, 225 (1971).

PHYSICAL REVIEW C VOLUME 6, NUMBER 3 SEPTEMBER 1972

Backward-Angle Elastic Scattering of ^{16}O on ^{40}Ca and ^{48}Ca†

K. O. Groeneveld,* L. Meyer-Schützmeister, A. Richter,‡ and U. Strohbusch§
Argonne National Laboratory, Argonne, Illinois 60439
(Received 7 April 1972)

Angular distributions at 40 MeV and backward-angle excitation functions in the energy range 25–45 MeV have been measured for ^{16}O elastic scattering on ^{40}Ca and ^{48}Ca. The ^{16}O + ^{40}Ca excitation function measured in this experiment shows no indication of the marked structure observed in earlier experiments and predicted by angular-momentum-dependent optical-model calculations. The experimental data are discussed by means of both the standard and the L-dependent optical models.

INTRODUCTION

Interest in the elastic scattering of ^{16}O has recently been stimulated in connection with an extension of the standard optical model to include an angular-momentum-dependent absorption.[1-6] This modification of the optical potential is expected to become important when orbital angular momenta carried into the nuclear region are larger than the maximum orbital momentum that can be carried away in any nonelastic channel. This results in increased transparency for the high-order partial waves. Introduction of an energy-dependent angular momentum cutoff for the absorptive potential has made possible an improved description of the experimental[7] ^{16}O + ^{16}O elastic scattering excitation functions[2] and of the ^{16}O + ^{40}Ca elastic scattering angular distributions[1] and has led to a better understanding of the pronounced differences between the ^{16}O + ^{16}O and ^{18}O + ^{18}O scattering.[5] The most striking result of this model has been the prediction[3] of strong resonance-like structures in the ^{40}Ca + ^{16}O elastic scattering excitation function at $\theta_{c.m.} = 180°$. Preliminary experimental results indeed seemed to show such resonances.[4] However, these results have now become questionable.[8,9]

We have therefore repeated the measurements on the elastic scattering of oxygen by ^{40}Ca and have extended them to ^{48}Ca. Excitation functions obtained at ~177° c.m. are presented and discussed in this paper. Angluar distributions have been

measured for ^{40,48}Ca(^{16}O, ^{16}O) at 40 MeV. The results are compared with optical-model calculations.

EXPERIMENTAL PROCEDURE AND RESULTS

The excitation functions were measured in a 4-in. scattering chamber at the Argonne FN tandem Van de Graaff. Thin targets (30 μg/cm^2 Ca on carbon backing) were bombarded with ^{16}O ions with energies from 25 to 45 MeV. The beam was aligned by observing the beam spot on a quartz viewer at the end of the beam line and was collimated by movable slits and apertures. The annular solid-state detector used was sufficiently thin to keep the proton groups out of the pulse-height region of interest. The detector subtended the angular range 176.7–178.0° c.m. In order to minimize the background due to backscattering, the beam stopper was placed far (3.5 m) from the detector.

The spectra included several α groups arising from the ^{12}C(^{16}O, α) reaction on the carbon backing in addition to the ^{16}O ions elastically scattered from Ca. The latter could easily be identified, however, by inspecting the movement of the various particle groups as a function of the bombarding energy. In addition, the oxygen group could be distinguished in the spectra from the α-particle groups by its larger energy spread (full width at half maximum). At energies at which the oxygen peak overlapped an α peak, the target was turned 180° so that the carbon layer faced the beam and the detector. Because of the large energy loss of the scattered oxygen ions in the carbon foil, the O peak was shifted to lower energies, while the α groups originating from the carbon foil shifted slightly to higher energies, as is demonstrated in Fig. 1. It was therefore possible to determine reliable backward-angle cross sections over the whole range of bombarding energies. Figure 2 shows the measured excitation function for ^{40}Ca. The cross sections were obtained by normalizing to the charge collected in the beam stopper, with proper correction for the energy dependence of the average charge of the oxygen ions that had passed through the target.[10] Absolute cross sections were determined by comparison with the Rutherford cross section at low energies. For energies $E \gtrsim 37$ MeV the points indicate an upper limit of 0.3 mb/sr, although these are the energies at which strong resonance structure were expected.[3,4] A curve similar to Fig. 2 is obtained for ^{16}O + ^{48}Ca.

Excitation functions for ^{40}Ca and ^{48}Ca are presented in Fig. 3. The curves represent the standard optical-model fits discussed below.

In addition to the excitation functions, angular distributions for ^{40}Ca + ^{16}O and ^{48}Ca + ^{16}O elastic scattering have been measured at 40 MeV in the angular range $\theta_{c.m.} = 15$–$110°$. The experimental results together with a standard optical-model calculation are shown in Fig. 4.

DISCUSSION

As Fig. 2 shows, there is no sign of the structures found earlier (Ref. 4) in the excitation function of the elastically scattered ^{16}O ions on ^{40}Ca for energies $E \gtrsim 37$ MeV. The structures reported in Ref. 4 most likely result from an α group arising from the ^{12}C(^{16}O, α) reaction. The yield of the α group which overlaps with the ^{16}O peak in the energy region of interest shows strong fluctuations parallel to the structures presented in Ref. 4.

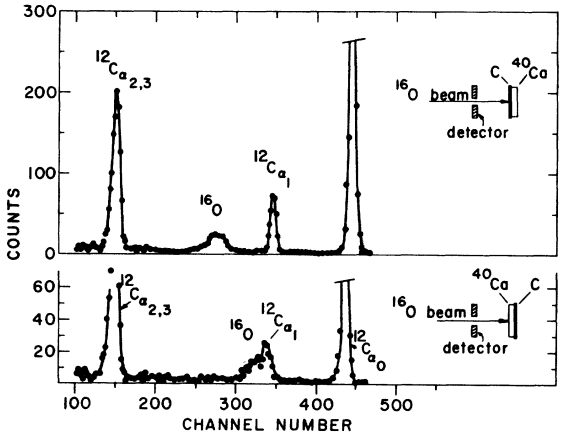

FIG. 1. Spectra obtained at $\theta_{lab} = 177°$ for the two indicated target positions. The broad peak labeled ^{16}O corresponds to ^{16}O + ^{40}Ca elastic scattering. The $^{12}C_{\alpha_i}$ peaks are due to the ^{12}C(^{16}O, α_i)^{24}Mg reaction leading to the ith excited state of ^{24}Mg.

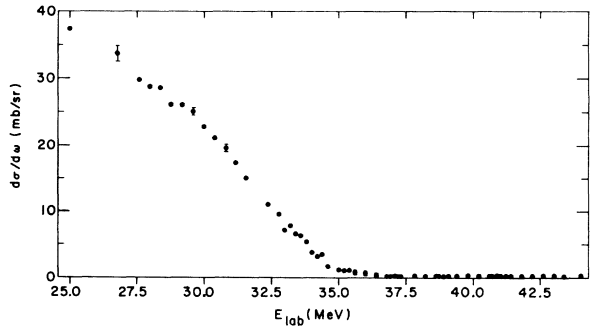

FIG. 2. Excitation function for ^{16}O + ^{40}Ca elastic scattering at $\theta_{lab} = 177°$.

We avoid this overlap by the technique indicated in Fig. 1. We have attempted to describe excitation functions, as well as angular distributions, with the help of the standard optical model.

The optical-model fits shown in Figs. 3 and 4 were obtained with the search code ABACUS.[11] In this search we used the four-parameter Woods-Saxon potential

$$U(r) = -(V + iW)(1 + e^{(r-R)/a})^{-1} + V_C(R_C, r), \qquad (1)$$

where V_C is the Coulomb potential resulting from a uniform charge distribution inside a sphere of radius R_C. The parameter search was started with the angular distribution for ^{48}Ca + ^{16}O. The initial parameters ($V = 100$ MeV, $W = 40$ MeV, $R = R_C = 7.3$ fm, and $a = 0.45$ fm) were similar to those used by Voos, von Oertzen, and Bock,[12] and an optimum fit (shown as the dashed curve in Fig. 4) was obtained for $W = 24.41$ MeV, $R = 7.43$ fm, and $a = 0.50$ fm. Since V is strongly correlated with R, it was kept fixed at $V = 100$ MeV. With these parameters the excitation function drawn in Fig. 3 (dashed line) was calculated. The curves through the ^{40}Ca + ^{16}O data (solid lines in Figs. 3 and 4) were obtained by merely changing the radius R to 7.25 fm. The radius thus appears to have the usual A dependence and is given by $R(\mathrm{Ca}) = 1.22 \times [16^{1/3} + A(\mathrm{Ca})^{1/3}]$.

The calculated cross sections were insensitive to changes in the Coulomb radius R_C; a variation of R_C from 7.0 to 7.7 fm produced no sizable effect on the calculated curves. This might seem surprising in view of the clear effect of small changes in the radius R of the nuclear potential. The reason for this insensitivity to R_C certainly is that the relevant part of the potential, the Coulomb barrier, is outside the assumed charge sphere. Both the Coulomb potentials V_C and the sum of V_C and the real nuclear potential V for ^{16}O + ^{40}Ca and for ^{16}O + ^{48}Ca are plotted in Fig. 5. The energy shift between the ^{40}Ca and the ^{48}Ca excitation function (Fig. 3) reflects the difference between the heights ($V_C + V$) of the two potential barriers.

Our data do not determine the optical parameters unambiguously. A change of ±0.1 fm in R could, for example, be compensated by a change of ∓0.02 fm in the diffuseness a without affecting the calculated results. It is beyond the purpose of this paper to investigate such ambiguities in detail, but the reader is referred to the papers of Robertson *et al.*[13] and of Orloff and Daehnick.[14] The elastic scattering of ^{16}O on $^{40, 44, 48}$Ca in the neighborhood of the Coulomb barrier has been discussed in more detail by Bertin *et al.*,[15] who pointed out that only two parameters are determined independently by such an analysis. The most appropriate pair of choices consists of the "Rutherford radius" R_R, i.e., the position of the maximum in the total potential $V(R) + V_C(R)$, and the function f defined by $f = 1 - R_R[V(R_R) + V_C(R_R)]/Z_1 Z_2 e^2$. Table I lists the optical-model parameters and also the values of R_R and f obtained here, together with those obtained in Ref. 15 for comparison.

Our data are well described by the standard optical model, and the excitation function shows no sign of the strong resonant structure predicted[3] by the angular-momentum-dependent optical potential. In the latter model, the imaginary part is assumed[1-3] to be of the form $W(r)g(J)$, where

$$g(J) = (1 + e^{(J-J_c)/\Delta J})^{-1}, \qquad (2)$$

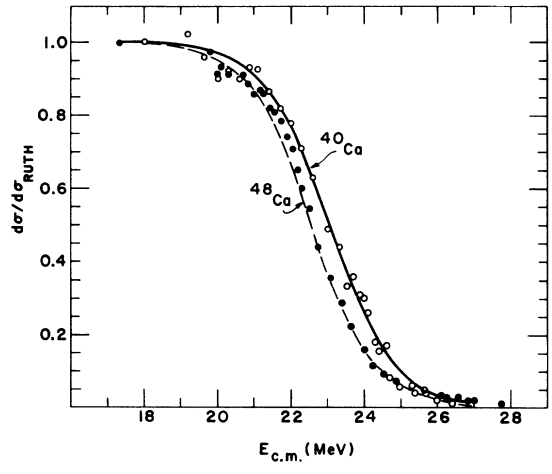

FIG. 3. Excitation functions for ^{16}O elastic scattering on ^{40}Ca and ^{48}Ca, normalized to the Rutherford-scattering cross section. The curves are standard optical-model fits with the parameters listed in Table I.

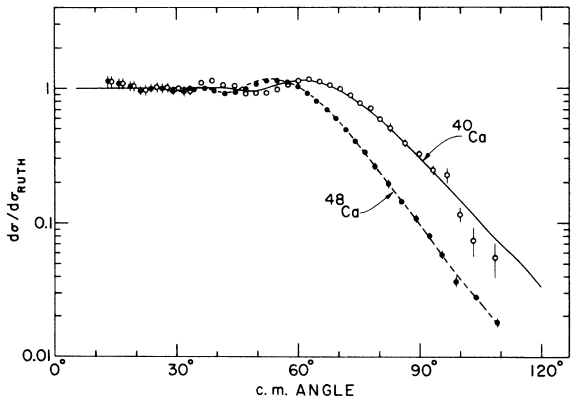

FIG. 4. Angular distributions for ^{16}O elastic scattering on ^{40}Ca and ^{48}Ca at $E_{lab}(^{16}\mathrm{O}) = 40$ MeV. The curves are standard optical-model fits with the parameters of Table I.

TABLE I. Optical-model parameters. For the definitions of R_R and f, see the text.

Target	V (MeV)	W (MeV)	R (fm)	a (fm)	R_R (fm)	$10^2 f$	Source
^{40}Ca	100	24.41	7.25	0.50	9.35	5.29	Present analysis
					9.250	5.65	Ref. 15
^{48}Ca	100	24.41	7.43	0.50	9.55	5.16	Present analysis
					9.662	4.87	Ref. 15

with $J = L$ for $^{16}O + ^{40}Ca$. This form factor takes account of the fact that the absorption of incident partial waves with L larger than a critical value L_c may be restricted because of a lack in exit channels with correspondingly high angular momentum. Clearly, this restriction becomes ineffective if the maximum orbital momentum L_{max} carried into the nuclear region (grazing orbital momentum) is smaller than L_c. Our data, which do not show the expected resonance structure, probably indicate that the orbital momentum cutoff chosen for the calculation of Refs. 1, 3, and 4 [$L_c = 11$–13 for $E_{lab}(^{16}O) = 38$–42 MeV] is too small.

To check how changes in L_c influence the calculated excitation function, we have calculated the backward scattering for $^{16}O + ^{40}Ca$ by use of the optical potential[16] whose form factor for the imaginary part $W(r)$ is as given in Eq. (2). The assumed energy dependence of L_c was the same as in Ref. 3, namely,

$$L_c = (2\mu/\hbar^2)^{1/2}\overline{R}(E + \overline{Q})^{1/2}, \quad (3)$$

where E is the c.m. energy, μ is the reduced mass, and $\overline{R}$ and $\overline{Q}$ are parameters representing average values of channel radius and effective threshold energy for nonelastic channels. The parameters of Table I were used for the real part of the potential as well as for $W(r)$, and $\overline{R}$ was set equal to R. The diffuseness parameter was taken to be $\Delta L = 0.5$ (as in Refs. 1, 3, and 4), and $\overline{Q}$ was varied to change the range of L_c. (Though the parameters – especially $\overline{R}$, $\overline{Q}$, and W – are functions of energy, it is sufficient for this qualitative discussion to use constant values as has been done in Refs. 3 and 4.) The results are displayed in Fig. 6. For $L_c = 7$–15 (thin solid curve) in the investigated energy region, the excitation function is similar to that obtained in Refs. 3 and 4. (Observed differences are partly due to the significantly larger depth of the real potential used here. The additional structure in our results arises from the smaller energy step.) The marked structure is considerably reduced when L_c is increased to 11–17 (dashed curve). The disappearance of

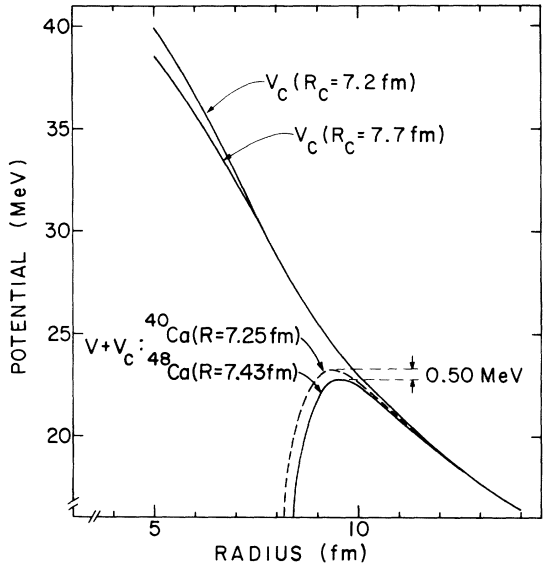

FIG. 5. Coulomb potentials V_c and the Coulomb-plus-real nuclear potentials used in the optical-model calculations which yield the fits shown in Figs. 3 and 4 (optical-model parameters given in Table I).

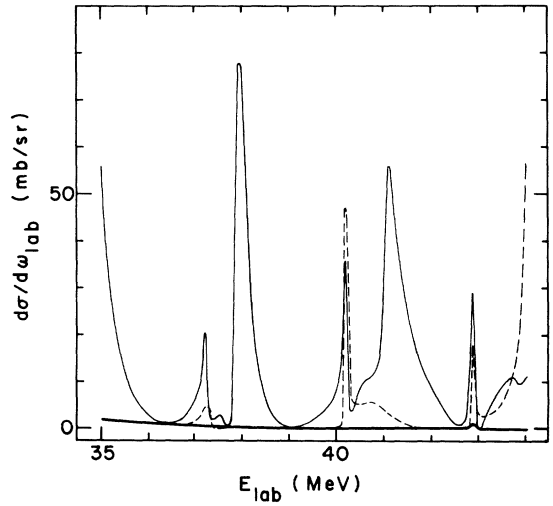

FIG. 6. Excitation functions for $^{16}O + ^{40}Ca$ elastic scattering at $\theta_{c.m.} = 178°$, calculated by use of an L-dependent absorptive potential. The thin solid line corresponds to an orbital momentum cutoff parameter in the range $L_c = 7$–15, the dashed curve to $L_c = 11$–17, and the heavy full curve to $L_c = 14$–19.

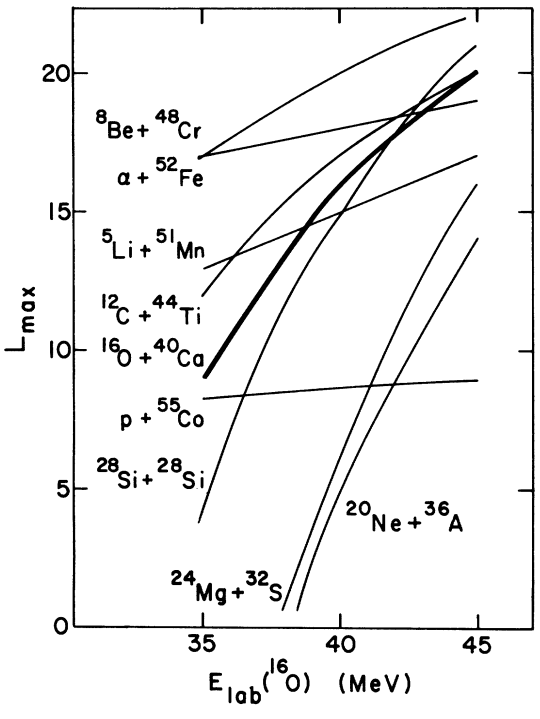

FIG. 7. Maximum orbital momenta L_{max} (the L value for which the transmission coefficient is 0.5) for $^{16}O + ^{40}Ca$ elastic scattering and for several connected exit channels (ground-state transitions) plotted as a function of the ^{16}O bombarding energy.

the structure when $L_c = 14-19$ (heavy curve) indicates that L_c is now larger than L_{max}.

In Fig. 7, L_{max} for the $^{16}O + ^{40}Ca$ elastic scattering channel, as well as for nonelastic channels, is plotted as a function of the oxygen bombarding energy. Here L_{max} is the L value for which the transmission coefficient T_L has fallen to 0.5. The transmission coefficients for all channels shown in Fig. 7 were calculated by use of the optical parameters of Table I, with $R = 1.22\ (A_1^{1/3} + A_2^{1/3})$. Since the transmission coefficients are rather insensitive to details of the optical potentials, the present purposes do not require the use of special measured potentials for the different channels. (A check with more realistic potential depths – e.g., with $V = 50$ and 150 MeV for the p and α channels, respectively, and $W = 8$ MeV for both – yielded the same transmission coefficients as were obtained with the potentials of Table I.)

As shown in Fig. 7, there are indeed several nonelastic channels that may carry out the maximum orbital momentum brought into the nuclear region by the $^{16}O + ^{40}Ca$ channel. Nonzero final spins will further increase the number of channels matching the angular momentum carried in. Figure 7 of course says nothing about the strength of the absorption into the open channels. As far as the direct mechanism is concerned, the "α"-transfer channel[17] $^{12}C + ^{44}Ti$ and perhaps the $^{8}Be + ^{48}Cr$ and $\alpha + ^{52}Fe$ channels are of importance and possibly contribute significantly to the absorption of the incoming surface waves. In order to take this into account, the cutoff L_c in the L-dependent form factor would have to be taken larger than L_{max} of the entrance channel. This implies that the elastic scattering is not affected by this form factor.

The situation for $^{48}Ca + ^{16}O$ is similar to that for $^{40}Ca + ^{16}O$ (the number of open channels is even larger for $^{48}Ca + ^{16}O$ than for $^{40}Ca + ^{16}O$). Hence no effect of L dependence is expected in this case either. This is supported by the experimental findings.

The above discussion, for the same reason as given by the authors of Ref. 5, disregards possible absorption into exit channel which result from compound nucleus formation.

The main results of this paper can be summarized as follows. Our data are well described by standard optical-model calculations. The strong resonant behavior predicted by an optical model with an angular-momentum-dependent absorptive part and which had been believed to be observed at $\theta_{c.m.} = 178°$ is not verified by this experiment. The cross section for $^{16}O + ^{40,48}Ca$ elastic scattering is smaller than 0.3 mb/sr in the energy range 37–45 MeV. Our data indicate that the form factor used in Refs. 1, 3, and 4 underestimated the absorption of high-order partial waves.

ACKNOWLEDGMENTS

We thank Y. Eisen, K. Katori, R. Malmin, D. Robson, and R. H. Siemssen for helpful discussions. We are grateful to N. Cornelius and S. Meyer for assistance in evaluation and analysis of the data, to S. Omiecinski for preparing the targets, and to the staff of the tandem for cooperation. One of us (U.S.) gratefully acknowledges the financial support by the Bundesministerium für Bildung und Wissenschaft, Germany.

†Work performed under the auspices of the U. S. Atomic Energy Commission.

*Present address: Institut für Kernphysik der Universität Frankfurt, Frankfurt, Germany.

‡Present address: Institut für Experimentalphysik der Ruhr-Universität Bochum, Bochum, Germany, and Max-Planck Institut für Kernphysik, Heidelberg, Germany.

§On leave from Physikalisches Institut der Universität Freiburg, Freiburg, Germany.

[1]J. S. Eck, R. A. LaSalle, and D. Robson, Phys. Rev. 186, 1132 (1969).

[2]R. A. Chatwin, J. S. Eck, D. Robson, and A. Richter, Phys. Rev. C 1, 795 (1970).

[3]R. A. Chatwin, J. S. Eck, A. Richter, and D. Robson, in *Nuclear Reactions Induced by Heavy Ions*, edited by R. Bock and W. Hering (North-Holland, Amsterdam, 1970), p. 76.

[4]J. S. Eck, R. A. Chatwin, K. A. Eberhard, R. A. LaSalle, A. Richter, and D. Robson, in *Nuclear Reactions Induced by Heavy Ions* (see Ref. 3), p. 80.

[5]R. W. Shaw, Jr., R. Vandenbosch, and M. K. Mehta, Phys. Rev. Letters 25, 457 (1970).

[6]G. Helling, W. Scheid, and W. Greiner, Phys. Letters 36B, 64 (1971).

[7]J. V. Maher, M. W. Sachs, R. H. Siemssen, A. Weidinger, and D. A. Bromley, Phys. Rev. 188, 1665 (1969); Phys. Rev. Letters 19, 968 (1967).

[8]D. Robson, Argonne National Laboratory Report No. ANL-7837, March 1971 (unpublished), p. 239.

[9]R. Vandenbosch, Argonne National Laboratory Report No. ANL-7837, March 1971 (unpublished), p. 103.

[10]L. C. Northcliffe, Phys. Rev. 120, 1744 (1960); R. E. Malmin, private communication.

[11]E. H. Auerbach, Brookhaven National Laboratory Report No. BNL-6562, 1962 (unpublished).

[12]U. C. Voos, W. von Oertzen, and R. Bock, Nucl. Phys. A135, 207 (1969).

[13]B. C. Robertson, J. T. Sample, D. R. Goosman, K. Nagatani, and K. W. Jones, Phys. Rev. C 4, 2176 (1971).

[14]J. Orloff and W. W. Daehnick, Phys. Rev. C 3, 430 (1971).

[15]M. C. Bertin, S. L. Tabor, B. A. Watson, Y. Eisen, and G. Goldring, Nucl. Phys. A167, 216 (1971).

[16]A revised version of code ABACUS was used. We are grateful to S. Zawadzki for making this revision.

[17]A. M. Friedman, H. T. Fortune, G. C. Morrison, and R. H. Siemssen, in *Nuclear Reactions Induced by Heavy Ions* (see Ref. 3); H. Faraggi, M.-C. Lemaire, J.-M. Loiseaux, M. C. Mermaz, and A. Papineau, Phys. Rev. C 4, 1375 (1971).

PHYSICAL REVIEW C VOLUME 6, NUMBER 3 SEPTEMBER 1972

^{96}Mo(p, xn) Reaction from 10 to 80 MeV*

James J. Hogan

Department of Chemistry, McGill University, Montreal, Quebec, Canada

(Received 20 March 1972)

Excitation functions for the ^{96}Mo(p,xn)$^{97-x}$Tc reactions have been measured for proton bombarding energies from 10–80 MeV. These experimental results have been compared to excitation functions calculated using the most recent version of intranuclear cascade model, that known as VPOT, as well as the older STEP. The two models are compared, particularly with reference to improvements in the newer, more sophisticated VPOT. This model provides substantially better agreement with experiment than STEP, although it is also found to introduce new problems.

INTRODUCTION

In recent years, much attention has been given to attempts to calculate the detailed mechanism of nuclear reactions induced by high-energy protons. Such a calculation requires two steps: first, production of an excited nucleus, and then, its decay. The second step, relaxation of the excited nucleus by evaporation of nucleons, may be calculated by means of the Dostrovsky, Fraenkel, and Friedlander[1] formalism. This is a purely statistical calculation which has been used to reproduce experimental data in a wide variety of nuclear reactions.[2]

Calculations of the initial interaction of bombarding proton and nucleus have provided qualitative, but not, in general, quantitative agreement with experimental excitation functions. Succeeding generations of Monte Carlo intranuclear-cascade calculations[3-7] have become increasingly sophisticated but have not always led to the expected improvement in agreement with experiment. A case in point is the most widely used of such calculations, that known as Vegas.[5] The Vegas calculation, in its simplest form called STEPNO, was found[5] to substantially improve agreement with experiment over previous calculations.[3,4] The chief advance of this calculation was inclusion